

## Dynamic light scattering of CTAB:NaSal threadlike micelles in the semidilute regime. II. effect of surfactant concentration

A. Koike, T. Yamamura, and N. Nemoto

Institute for Chemical Research, Kyoto University, Japan

**Abstract:** Dynamic light scattering measurements are made on networks formed by elongated threadlike micelles of cetyltrimethylammonium bromide (CTAB) in aqueous sodium salicylate (NaSal) solutions at 25 °C. The surfactant concentration  $C_D$  of the samples is varied from 0.006 to 0.3 M and the ratio of the salt concentration  $C_s$  to  $C_D$  is fixed at unity. The time correlation function  $A_q(t)$  of light intensity scattered from the solutions exhibits transition from the unimodal to the bimodal distribution of the decay rate  $\Gamma$  at around  $C_D = 0.05$  M. The dependence of the first cumulant  $\Gamma_c$  on the scattering vector  $q$  for the samples with  $C_D \leq 0.03$  M is described by the dynamic scaling law. The cooperative diffusion coefficient  $D_c$  is obtained from extrapolation of  $\Gamma_c/q^2$  for the samples with  $C_D \leq 0.03$  M and of  $\Gamma_t/q^2$  for  $C_D \geq 0.05$  M where  $\Gamma_t$  is the first cumulant from the fast mode. The  $D_c$  is found in proportion to  $C_D^{0.45}$ , being in agreement with the theoretical prediction for a rigid rod in the semidilute regime by the scaling law. The decay rate  $\Gamma_s$  characteristic of the slow mode is independent of  $q$ , and  $\Gamma_s^{-1}$  roughly agrees with the mechanical relaxation time  $\tau$  estimated from a fit of the dynamic viscoelastic data of the same samples by a Maxwell type of model with the single relaxation time  $\tau$ .

**Key words:** Dynamic light scattering – CTAB:NaSal micelles – semidilute regime – cooperative diffusion coefficient – first cumulant – relaxation mode

### Introduction

It is well established by an electron microscopic observation that cetyltrimethylammonium halide, CTAX (X = B for bromide and C for chloride), forms a long threadlike micelle in aqueous sodium salicylate (NaSal) solution [1,2]. The CTAX:NaSal micelles, being stabilized by formation of a 1:1 complex of  $CTA^+$  and  $Sal^-$  ions, form a network at low CTAX concentration  $C_D$ , and exhibit viscoelastic properties [2–7] quite distinct from those observed for an entanglement network of flexible high molecular weight polymer chains [8–11].

In an earlier forced Rayleigh scattering study of the CTAB:NaSal/W system (W stands for water) [12], we showed that the translational diffusion coefficient  $D$  of a micelle in the network was dependent on both  $C_D$  and a ratio of salt concentration  $C_s$  to  $C_D$  in a complicated manner. The

$D$  took a maximum with increasing  $C_D$  at  $C_s/C_D = 1$ , and at a fixed  $C_D$  with increasing  $C_s/C_D$ ,  $D$  took a maximum which is followed by a minimum. Dependencies of the relaxation time  $\tau$  on both  $C_D$  and  $C_s/C_D$  estimated from a fit of the dynamic shear modulus data by a Maxwell type of model with the single relaxation time  $\tau$  were found consistent with the diffusion behavior. Those slow molecular motions specific for this micellar system were interpreted in terms of the non-topological network model [4] and the rigid rod model in the semidilute regime [12,13].

Dynamic light scattering (DLS) experiments were also performed to study faster molecular motions in the same micellar systems [14–16]. The discussion is mainly focused on dependencies of the cooperative (or the gel) diffusion coefficient  $D_c$  on  $C_D$ ,  $C_s/C_D$  and temperature  $T$ . Candau and his groups showed that the behavior was very close to those predicted for semidilute polymer

solutions as was already found for the CTAB:KBr/W system [17,18]. Imae [15] and also Ng et al. [16], on the other hand, interpreted their data based on the formation of pseudo-linkages and entanglement couplings among micelles. Very recently, we performed DLS measurements on networks composed of the threadlike CTAB:NaSal micelles with low surfactant concentration of  $C_D = 0.01$  M for an estimate of the first cumulant  $\Gamma_e$  as a function of the scattering vector  $q$ ,  $C_s/C_D$  and  $T$  [19]. We showed that  $D_c$  and the dynamic correlation length  $\xi_H$  were dependent on  $C_s/C_D$  in a complicated manner, while they monotonically changed with  $T$ . In making a reduced plot of  $\Gamma_e/q^2 D_c$  vs  $q \xi_H$ , all  $\Gamma_e$  data for the samples with  $C_s/C_D = 1 - 41$  at three temperatures were superposed on one master curve, which was in close agreement with the theoretical prediction developed for chain dynamics of linear flexible macromolecules in the semidilute regime. The  $q^3$  dependence of  $\Gamma_e$  was also found on DLS behavior of threadlike micelles from cetylpyridinium chloride in aqueous sodium chlorate solutions [20].

This paper describes results of DLS measurements on CTAB:NaSal/W system over the wide range of  $C_D$  from 0.006 to 0.3 M at a fixed  $C_s/C_D$  value of unity. As Brown et al. found for threadlike micelles from CTAB in aqueous sodium chlorate solutions [21], time profiles of the autocorrelation function  $A_q(t)$  of light intensity scattered from our samples indicated that the distribution of the decay rate changed from a unimodal to a bimodal one at a threshold value of  $C_D = 0.05$  M. We shall discuss the  $q$  dependence of the first cumulant  $\Gamma_e$ ,  $C_D$  dependence of  $D_c$ , and of the  $q$ -independent  $\Gamma_s^{-1}$  from the slow mode at higher  $C_D$  with earlier viscoelastic data.

## Experimental

### Materials

Twice-recrystallized cetyltrimethylammonium bromide (CTAB) (Nacalai Tesque) and special-grade sodium salicylate (NaSal) (Nacalai Tesque) were chosen in this study as cationic surfactant and salt samples, respectively. Dust-free purified water (resistance  $> 16$  M  $\Omega$ ) was used as solvent. The samples were prepared by mixing prescribed

amounts of aqueous solutions of CTAB and of NaSal and by equilibrating at room temperature for at least 2 days. The surfactant concentrations  $C_D$  of 10 solutions tested were 0.006, 0.01, 0.02, 0.03, 0.05, 0.07, 0.1, 0.15, 0.2, and 0.3 M, and a ratio of the salt concentration  $C_s$  to  $C_D$  was fixed at unity. The solutions were made optically clean by filtering with a Millipore filter (nominal pore size,  $0.22 \mu\text{m}$ ) for dynamic light scattering (DLS) and equilibrated in dynamic light scattering cells for about 1 week.

### Methods

Dynamic light scattering measurements were made with an instrument reconstructed in our laboratory. Details of the instrument are given elsewhere [19]. A vertically polarized single frequency 488 nm line of an argon ion laser (Spectra Physics, Model 165-03) was used as a light source with an output power of 300 mW. The normalized auto correlation function  $A_q(t)$  of the vertical component of the light intensity  $I(t)$  scattered from the solutions was measured using the digital correlator (Malvern, 72 channels) at eleven fixed scattering angles ranging from  $10.4$  to  $150^\circ$ . The experiments were conducted at  $T = 25^\circ\text{C}$ .

## Results and discussion

### Time profiles of $A_q(t)$

In the range of  $0.006 \text{ M} \leq C_D \leq 0.03 \text{ M}$ , the time correlation function  $A_q(t)$  of the CTAB:NaSal micellar solutions showed the unimodal distribution of the decay rate. An example is shown in Fig. 1 for the solution with  $C_D = 0.02 \text{ M}$  at the scattering angle  $\theta = 60^\circ$ . Since  $A_q(t)$  could not be fitted to the single exponential type of a decay function at any scattering angle, we applied the cumulant method to estimate the first cumulant  $\Gamma_e$ .

$$A_q(t) = 1 + A_1 |g_q^{(1)}(t)|^2 \quad (1)$$

$$\ln |g_q^{(1)}(t)| = \sum K_m(\Gamma_q) (-t)^m/m! \quad (2)$$

$$\Gamma_e = K_1(\Gamma_q) \quad (3)$$

Here,  $A_1$  is the amplitude and  $g_q^{(1)}(t)$  is the time correlation function of the scattered electric field. The fitted curve shown as the solid curve in Fig. 1

is a result obtained with the fourth order cumulant fitting (the variance  $\sim 0.1$ ). Randomness of small residuals given at the bottom of the figure indicates that  $\Gamma_e$  is obtained to an accuracy of 10%.

Figure 2 gives a typical example of  $A_q(t)$  observed for the CTAB:NaSal solutions with higher

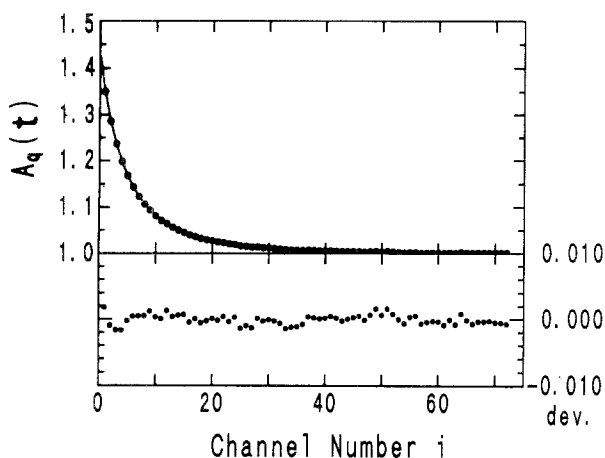
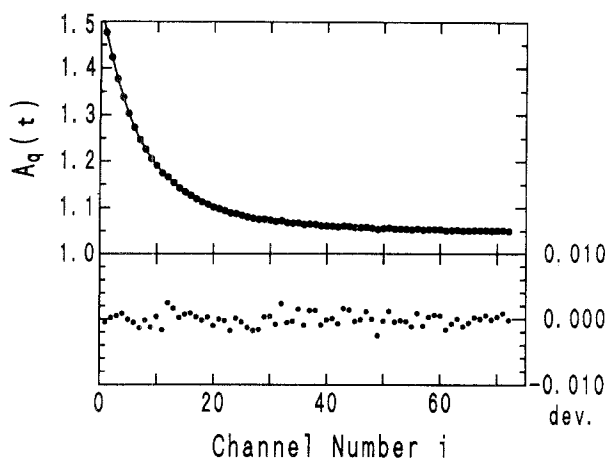


Fig. 1. A time profile of  $A_q(t)$  for the sample with low surfactant concentration of  $C_D = 0.02$  M and  $C_s/C_D = 1$  at  $\theta = 60^\circ$  as an example of when the decay rate distribution is unimodal. The sampling time  $\Delta\tau$  is  $60 \mu\text{s}$ . The fourth-order cumulant fittings shown by the solid curve gives  $\Gamma_e = 1.76 \times 10^3 \text{ s}^{-1}$  with small random residuals given at the bottom of the figure.



surfactant concentration of  $C_D \geq 0.05$  M to which the decay rate distribution is found bimodal. Since the channel number of our correlator is only 72, we measured  $A_q(t)$  repeatedly by varying the sampling time  $\Delta\tau$  by more than two orders of magnitude to cover the broad range of  $\Gamma$ . The  $A_q(t)$  curves in Fig. 2 are obtained for the sample with  $C_D = 0.3$  M at the same scattering angle of  $\theta = 10.4^\circ$  with  $\Delta\tau = 200 \mu\text{s}$  (a) and  $\Delta\tau = 40 \text{ ms}$  (b). As is clear from the figure, the fast and the slow modes are well separated in time scale, so that the first cumulants  $\Gamma_f$  and  $\Gamma_s$  ( $\Gamma_f \gg \Gamma_s$ ) can be estimated from the application of the cumulant analysis to respective curves in Figs. 2(a) and (b). The variance was found 0.1 and 0.05 – 0.15 for the fast and the slow mode, respectively. However, the amplitude  $A_s$  of the slow mode decreased with an increase in  $\theta$ , thus  $\Gamma_s$  could not be estimated at  $\theta$  larger than  $30^\circ$ . Within this limited  $q$  range,  $\Gamma_s$  was found independent of  $q$ , which indicates that the slow mode is not the diffusion mode but the relaxation mode.

#### The dependence of $\Gamma_e$ and $\Gamma_f$ on the scattering vector $q$

Figure 3 gives the  $q$  dependence of  $\Gamma_e/q^2$  for the solutions with  $C_D \leq 0.03$  M. The  $\Gamma_e/q^2$  shows strong  $q$  dependence at the two lowest surfactant concentrations, but becomes weakly dependent of

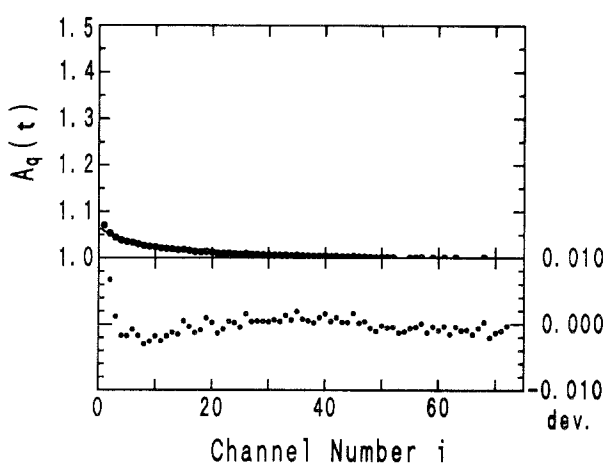


Fig. 2. Time profiles of  $A_q(t)$  for the sample with the highest concentration of  $C_D = 0.3$  M and  $C_s/C_D = 1$  at  $\theta = 10.4^\circ$  as an example of when the  $\Gamma$  distribution is bimodal. The sampling time  $\Delta\tau$  is a)  $200 \mu\text{s}$ , and b)  $40 \text{ ms}$ . The fourth-order cumulant fitting shown as the solid curve to each figure gives a value of a)  $\Gamma_f = 3.46 \times 10^2 \text{ s}^{-1}$ , and b)  $\Gamma_s = 9.51 \times 10^{-1} \text{ s}^{-1}$ , respectively.

$q$  at  $C_D = 0.02$  and  $0.03$  M. The cooperative diffusion coefficient  $D_c$  is estimated from extrapolation of  $\Gamma_e/q^2$  to the zero scattering vector, and the hydrodynamic correlation length  $\xi_H$  may be conveniently calculated using the Stokes-Einstein relation,

$$\xi_H = k_B T / 6 \pi \eta_m D_c. \quad (4)$$

Here,  $\eta_m$  should be, in a strict sense, considered as the viscosity of NaSal-Water mixtures [19], but is essentially the same as the viscosity of water at low  $C_s$ . Values of  $D_c$  and  $\xi_H$  are given in Table 1.

The  $q$  dependence of  $\Gamma_e/q^2$  may be ascribed to the intramolecular relaxation modes of network strands. In an earlier DLS study on CTAB:NaSal micellar networks with  $C_D = 0.01$  M and various  $C_s/C_D$  values from 1 to 41 [19], we showed that the reduced plot of  $\Gamma_e/q^2 D_c$  against  $q \xi_H$  gave one composite curve for all data measured at  $T = 25$ ,

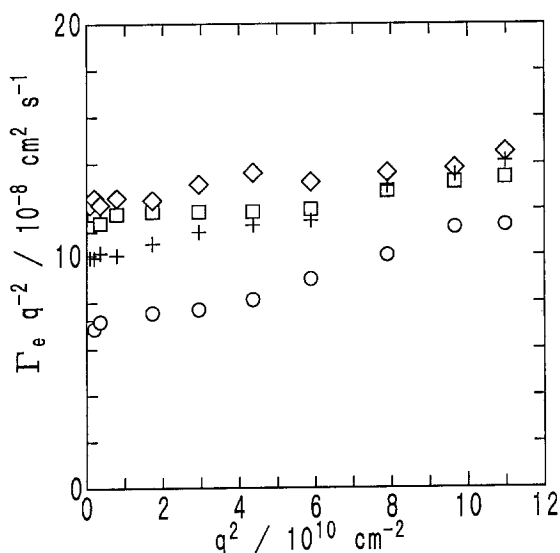


Fig. 3. A plot of  $\Gamma_e/q^2$  against  $q^2$  for the samples of which  $A_q(t)$  shows the unimodal distribution of the decay rate. Symbols for  $C_D$  are (○) 0.006 M, (+) 0.01 M, (□) 0.02 M, and (◇) 0.03 M.

33, 40 °C. The  $\Gamma_e/q^2$  data in Fig. 3 are reduced in exactly the same manner using  $D_c$  and  $\xi_H$  values listed in Table 1, and are plotted in Fig. 4 with the earlier data. Excellent superposition indicates that the dynamic scaling law is valid for the data obtained for the CTAB:NaSal solutions of different surfactant concentration.

The solid curve in the figure is the theoretical prediction for chain dynamics of linear flexible polymers in the semidilute regime.

$$\Gamma_e/q^2 D_c = F(q \xi_H) \quad (5)$$

$$F(x) = (3/4x^2) \{1 + x^2 + (x^3 - x^{-1}) \tan^{-1} x\} \quad (6)$$

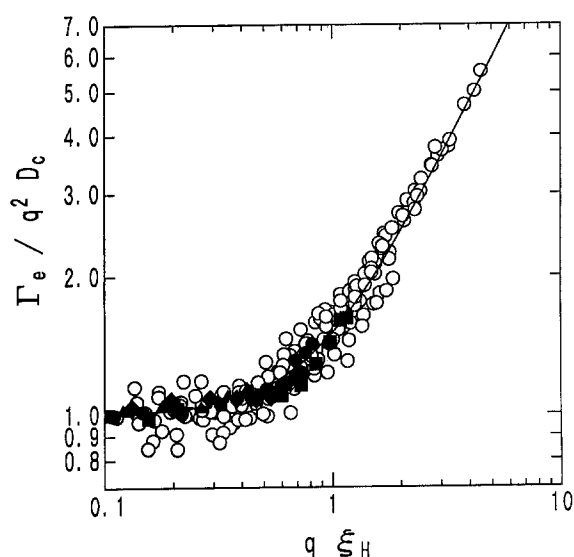


Fig. 4. The data in Fig. 3 are replotted in the reduced form of  $\Gamma_e/D_c q^2$  vs  $q \xi_H$  to test the applicability of the dynamic scaling law for surfactant concentration reduction. The  $D_c$  is estimated as  $(\Gamma_e/q^2)_{q \rightarrow 0}$  and  $\xi_H$  calculated using Eq. (4). Symbols are (○)  $C_D = 0.01$  M,  $C_s/C_D = 1 - 41$  and  $T = 25, 33$  and 40 °C (ref. [19]), (●)  $C_D = 0.006$  M and  $C_s/C_D = 1$ , (■)  $C_D = 0.02$  M and  $C_s/C_D = 1$ , and (◆)  $C_D = 0.03$  M and  $C_s/C_D = 1$ . The solid curve is the theoretical prediction of Eqs. (5) and (6).

Table 1.  $D_c$  and  $\xi_H$  of aqueous solutions of CTAB:NaSal threadlike micelles at  $C_s/C_D = 1$  and  $T = 25$  °C.

$C_D/\text{M}$	$D_c/10^{-8} \text{ cm}^2 \text{ s}^{-1}$	$\xi_H/\text{nm}$	$C_D/\text{M}$	$D_c/10^{-8} \text{ cm}^2 \text{ s}^{-1}$	$\xi_H/\text{nm}$
0.006	9.9	25	0.07	19	13
0.01	7.3	33	0.1	21	12
0.02	11	22	0.15	25	9.3
0.03	13	19	0.2	27	8.5
0.05	17	14	0.3	38	5.8

The curve has been originally derived for critical dynamics of low molecular weight liquids by Kawasaki [22]. Imae reported that the micelles obtained from recrystallization of aqueous solutions of CTAB and NaSal was short and rod-like in dilute solution, and took a long wormlike shape with the persistence length of about 140 nm in 0.1 M NaSal [15]. Thus, the agreement between the  $\Gamma_e/q^2 D_e$  vs  $q\xi_H$  plot and the theoretical curve does not necessarily mean that the CTAB:NaSal micelle is as flexible as a Gaussian polymer chain. Electrophoretic light-scattering measurements indicate that the micelles are positively charged at  $C_s/C_D = 1$  [23]. Therefore, a number of salicylate anions are present as free ions in water. The adsorption-desorption kinetics of these anions on the micelle surfaces may give rise to local fluctuation of charge density. The electrostatic force may then induce local bending motions to some extent. This kind of motion is possibly responsible for the  $q^3$  dependence of  $\Gamma_e$  for  $q\xi_H \gg 1$ .

Figure 5 shows the  $q$  dependence of  $\Gamma_f/q^2$  for the solutions with  $C_D \geq 0.05$  M. As is clear from the figure,  $\Gamma_f/q^2$  of all solutions is independent of  $q$  to an accuracy of 10%. Thus,  $D_e$  and  $\xi_H$  characteristic of the micellar network are easily estimated and are tabulated in Table 1. The  $\xi_H$

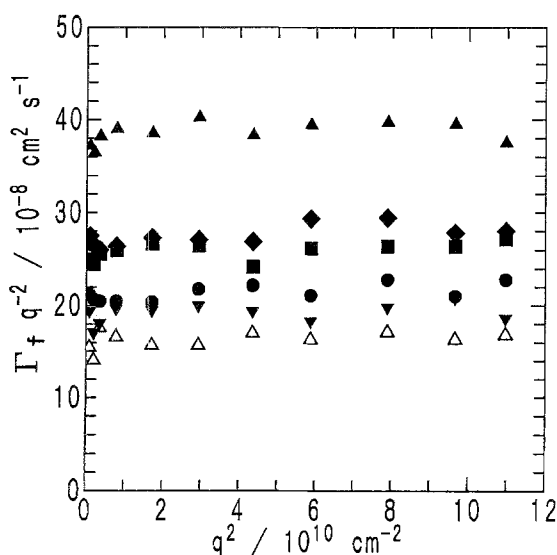


Fig. 5. The decay rate  $\Gamma_f$  from the fast mode of  $A_q(t)$  of the solutions which show the bimodal distribution of the decay rate is plotted in the form of  $\Gamma_f/q^2$  vs  $q^2$ . Symbols for  $C_D$  are ( $\Delta$ ) 0.05 M, ( $\nabla$ ) 0.07 M, ( $\bullet$ ) 0.1 M, ( $\blacksquare$ ) 0.15 M, ( $\blacklozenge$ ) 0.2 M, and ( $\blacktriangle$ ) 0.3 M.

decreases with increasing  $C_D$ , so that  $q\xi_H$  of the samples is about equal to or less than unity in the  $q$  range covered by DLS. This may explain the proportionality of  $\Gamma_f$  to  $q^2$  over the whole range of  $q$  studied.

#### Dependence of $D_e$ on $C_D$

Figure 6 is a logarithmic plot of  $D_e$  against  $C_D$ . The  $D_e$  first decreases with an increase in  $C_D$  and then increases in proportion to  $C_D^{0.45}$  in the range of  $0.3 \text{ M} \geq C_D \geq 0.01 \text{ M}$ . Makhoulfi et al. [14] have reported that  $D_e$  of CTAC with  $C_s/C_D = 0.6$  in the presence of 0.1 M NaCl exhibits a minimum at round  $C_D = 0.01 \text{ M}$  and obeys the power law of  $D_e \propto C_D^{0.77}$  at higher  $C_D$ . The exponent 0.77 is close to that predicted for semidilute polymer solutions in good solvent. They claim that the minimum reflects the crossover from the dilute range to the semidilute range where the elongated micelles form an entanglement network. This agreement is, however, not in harmony with the well-established fact that the diffusion coefficient of polymer chains in good solvent always monotonically increases in the crossover region from the dilute to the semidilute state. Dynamic viscoelastic measurements on our CTAB:NaSal/W system with  $C_s/C_D = 1$  show that the storage shear modulus has the pseudo-plateau region above  $C_D = 0.006 \text{ M}$ . This indicates that the network is already formed above this concentration by either pseudo-linkages between micelles or by

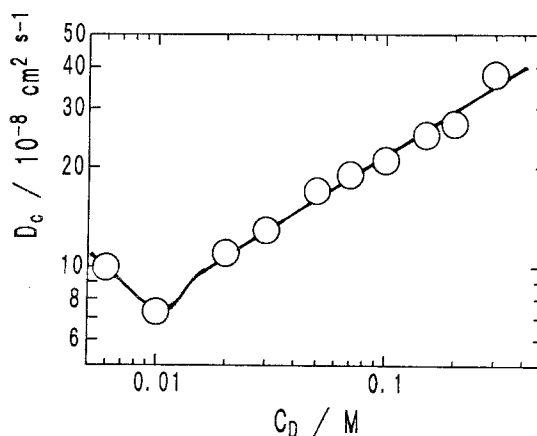


Fig. 6. The  $C_D$  dependence of the cooperative diffusion coefficient  $D_e$  obtained from extrapolation of  $\Gamma_e/q^2$  (Fig. 3) and  $\Gamma_f/q^2$  (Fig. 5) to the zero scattering vector.

topological constraints due to overlapping of micelles, i.e., entanglements. Therefore, the minimum observed for our system does not correspond to the crossover from the dilute to the semidilute region, but may be attributed to stiffening of the elongated micelles with increasing  $C_D$ .

Let us apply the dynamic scaling law with a form of Eq. (7) to predict the concentration dependence of  $D_e$ .

$$D_e = D_o (C_D/C_D^*)^\alpha \quad (7)$$

$D_o$  is usually taken as the translational diffusion coefficient of an isolated chain in the dilute region for the polymer solution [24]. If the CTAB:NaSal micelles in the extensively overlapped state are assumed to take a rodlike shape of length  $L$  independent of  $C_D$ ,  $D_o$  may be proportional to  $\ln(L/d)/L$  according to the diffusion theory for a rodlike polymer [13]. Here,  $d$  is the rod diameter. Since the threshold concentration  $C_D^*$  of the rigid rod with constant  $L$  is proportional to  $L^{-2}$ , a request of that  $D_e$  should only be a function of concentration gives a value close to 0.45 as the exponent  $\alpha$ , which slightly varies as the ratio of  $L/d$ . The above estimate is very crude and the agreement might be fortuitous. When the CTAB:NaSal micelle is considered to be better represented by a wormlike chain, variations in  $L$  and the persistence length with  $C_D$  may possibly explain the dependence of  $D_e$  on  $C_D$ . However,  $\alpha = 0.45$  is much smaller than  $0.75 - 1.0$  observed for flexible chains in the semidilute region and is only attainable from the assumption of the rodlike shape on the CTAB:NaSal micelle, as long as we use the theory of semidilute polymer solutions. It is noteworthy that an increase in the rod length with  $C_D$  following an expression like  $L(C_D) = L(C_D^*) (C_D/C_D^*)^\beta$  gives a larger value of  $\alpha = 0.5 + \beta$ .

*The slow mode for  $C_D \geq 0.05$  M*

We could unambiguously estimate the decay rate  $\Gamma_s$  from the slow mode for four samples with  $C_D = 0.1 - 0.3$  M. The amplitude of the slow mode for the lower  $C_D$  samples became so small above  $\theta = 20^\circ$ , and the independence of  $\Gamma_s$  on  $q$  could not be confirmed. Figure 7 gives a comparison of  $\Gamma_s^{-1}$  with the mechanical relaxation time  $\tau$  obtained from earlier dynamic viscoelastic measurements on the same samples [4, 5]. The latter was estimated from a fit of dynamic shear

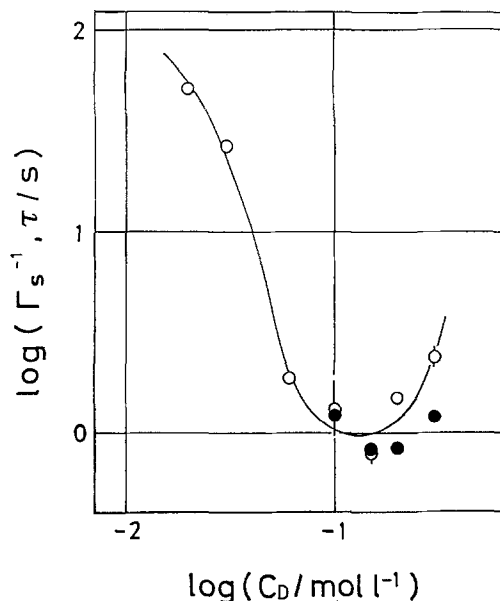


Fig. 7. The inverse of  $\Gamma_s$  from the slow mode observed in  $A_q(t)$  for the samples with  $C_D = 0.1, 0.15, 0.2$ , and  $0.3$  M is compared with  $\tau$  obtained from dynamic viscoelastic measurements on the same samples. Symbols are (●)  $\Gamma_s^{-1}$  and (○)  $\tau$ .

modulus data with a Maxwell model of the single relaxation time  $\tau$ . The data of the two samples with  $C_D = 0.1$  and  $0.15$  M agree well with each other, and  $\tau$  is larger than  $\Gamma_s^{-1}$  for the two higher  $C_D$  samples by a factor of about 2. The difference might be ascribed to a slight difference in the method of sample preparation.

Brown et al. detected the slow mode with a  $q$ -independent decay rate  $\Gamma_s$  for CTAB micelles in aqueous solutions containing either sodium naphthalene sulfonate or NaSal [21]. The dependence of  $\Gamma_s^{-1}$  on the concentration  $C^*$  of free salicylate ions  $\text{Sal}^-$  in water was found to be quite similar to that of  $\tau$  on  $C^*$  reported by Shikata et al. [4]. They have suggested that the two methods, DLS and dynamic viscoelasticity, both prove the same disruption/coalescence kinetics of the micellar aggregates. Substantial difference in absolute magnitude between  $\tau$  and  $\Gamma_s^{-1}$ , however, seems to make their conclusion ambiguous to some extent. Very recently, we have made DLS and dynamic viscoelastic experiments on the CTAB:NaSal/W system with  $C_D = 0.1$  M prepared by exactly the same procedure over the wide range of  $C_s/C_D$  and  $T$ . Good agreement between  $\Gamma_s^{-1}$  and  $\tau$  indicates that coupling between concentration fluctuation

and viscoelastic force definitely exists for our micelle system. A report on details of the study is in preparation.

#### Acknowledgment

This work is partly supported by a Grant-in-Aid for Scientific Research (No. 03453113) of the Ministry of Culture, Science and Education of Japan.

#### References

1. Shikata T, Sakaiguchi Y, Uragami H, Tamura A, Hirata H (1987) *J Colloid Interface Sci* 119:291
2. Clausen TM, Vinson PK, Minter JR, Davis HT, Talman Y, Miller WG (1992) *J Phys Chem* 96:474
3. Shikata T, Hirata H, Kotaka T (1987) *Langmuir* 3: 1081
4. Shikata T, Hirata H, Kotaka T (1988) *Langmuir* 4:354
5. Yamamura T, Kusaka T, Takatori E, Inoue T, Nemoto N, Osaki K, Shikata T, Kotaka T (1991) *Nihon Reoroji Gakkaishi* 19:45 (in Japanese).
6. Kern F, Zana R, Candau SJ (1991) *Langmuir* 7:1344
7. Hashimoto K, Imae T, Nakazawa K (1992) *Colloid Polym Sci* 270:249
8. Nemoto N, Kishine M, Inoue T, Osaki K (1990) *Macromolecules* 23:659
9. Nemoto N, Kishine M, Inoue T, Osaki K (1991) *Macromolecules* 24:1648
10. Nemoto N (1990) In Collyer AA, Utracki LA (eds) *Polymer Rheology and Processing*, Elsevier:London pp 3
11. Lodge TP, Rotstein NS, Prager S (1990) *Adv Chem Phys* 79:1
12. Nemoto N, Yamamura T, Osaki K, Shikata T (1991) *Langmuir* 7:2607
13. Doi M, Edwards SF (1986) *The Theory of Polymer Dynamics*, Oxford University Press:Oxford
14. Makhloufi R, Hirsch E, Candau SJ (1989) *J Phys Chem* 93:8095.
15. Imae T (1990) *J Phys Chem* 94:5953
16. Ng SC, Gan LM, Chew CH (1992) *Colloid Polym Sci* 270:64
17. Candau SJ, Hirsch E, Zana R (1985) *J Colloid Interface Sci* 105:521
18. Candau SJ, Hirsch E, Zana R, Adam M (1988) *J Colloid Interface Sci* 122:430
19. Nemoto N, Kuwahara M (1993) *Langmuir* 9:419
20. Appell J, Porte G (1990) *Europhys Lett* 12:185
21. Brown W, Johansson K, Almagren M (1989) *J Phys Chem* 93:5888
22. Kawasaki K (1971) In Green MS (eds) *Critical Phenomena*, Academic Press:New York pp 342
23. In preparation
24. De Gennes PG (1976) *Scaling Concepts in Polymer Physics*, Cornell University Press:New York

Received April 22, 1993  
accepted October 8, 1993

Authors' address:  
Prof. Dr. Norio Nemoto  
Institute for Chemical Research, Kyoto University  
Uji, Kyoto 611 Japan